Invited Paper

Optical immunoassay systems based upon evanescent wave interactions

Douglas A. Christensen and James N. Herron

Dept. of Bioengineering and Dept. of Electrical Engineering
University of Utah, Salt Lake City, Utah 84112

ABSTRACT

Immunoassays based upon evanescent wave interactions are finding increased biosensing application. In these devices, the evanescent tail associated with total internal reflection of an incident beam at the substrate/solution interface provides sensitivity for surface-bound proteins over bulk molecules, allowing homogeneous assays and real-time measurement of binding dynamics. Among such systems are surface plasmon resonance sensors and a resonant mirror device. Several research groups are also developing fluorescent fiberoptic or planar waveguide sensors for biomedical applications. We describe a second-generation planar waveguide fluoroimmunoassay system being developed in our laboratory which uses a molded polystyrene sensor. The 633-nm beam from a laser diode is focused into the 500 μm-thick planar waveguide by an integral lens. Antibodies to the desired analyte (hCG) are immobilized on the waveguide surface and fluorescence from bound analyte/tracer antibodies in a sandwich format is imaged onto the detector. The geometry of the waveguide allows several zones to be detected, providing the capability for on-sensor calibration. This sensor has shown picomolar sensitivity for the detection of hCG.

Keywords: Immunoassays, biosensors, diagnostics, evanescence, waveguides

1. INTRODUCTION

Surfaces are of primary importance in many of today's biosensing and biochemical analysis techniques.[1] For example, solid-phase immunoassays rely upon the binding of an analyte being measured to its antibodies which have been immobilized on the surface of a solid structure. The environment immediately surrounding the binding surface plays a major role in determining the sensitivity of the analysis technique.

Optical biosensors use light to probe this local environment. If the incident light is passed through a transparent dielectric layer forming the antibody-support surface, at large enough angles of incidence the beam will be totally internally reflected (TIR) from the dielectric/solution interface. Under this condition, a certain nonpropagating portion of the incident wave penetrates a short distance (typically much less than a wavelength) into the binding region of the solution. Although short, the penetration depth of this evanescent tail is larger than the thickness of the binding layer (typically 10-20 nm) and therefore it acts as a probe for optical changes--such as index of refraction, absorption, or the presence of fluorescent labels--taking place in the binding region.

This paper first describes the evanescent behavior of the electric field under conditions of TIR, then discusses some examples of optical biosensor techniques that exploit this behavior, including a surface plasmon resonance system and a resonant mirror device. The paper then covers in some detail the development in our laboratory of a planar waveguide fluorescent immunoassay system which also relies upon evanescent wave interactions in the binding layer.

2. TOTAL INTERNAL REFLECTION AND EVANESCENCE

Consider an electromagnetic wave with a free-space wavelength λ incident upon a dielectric/water interface at an angle ϕ, as shown in Fig. 1. For the case considered here, the polarization of the electric field is parallel to the interface, i.e., a transverse electric (TE) mode (this polarization maximizes the fluorescence radiation pattern in the x direction). The wave inside the dielectric layer of refractive index n_2 has a sinusoidal transverse variation of its electric field given by[2]

$$E_2 \propto A\, e^{jhx} + B\, e^{-jhx} \tag{1}$$

By using Maxwell's wave equation, the transverse propagation constant h inside this region can be related to the free-space propagation constant $k=2\pi/\lambda$ and the longitudinal propagation constant β, where β is given by

0-8194-2054-9/96/$6.00

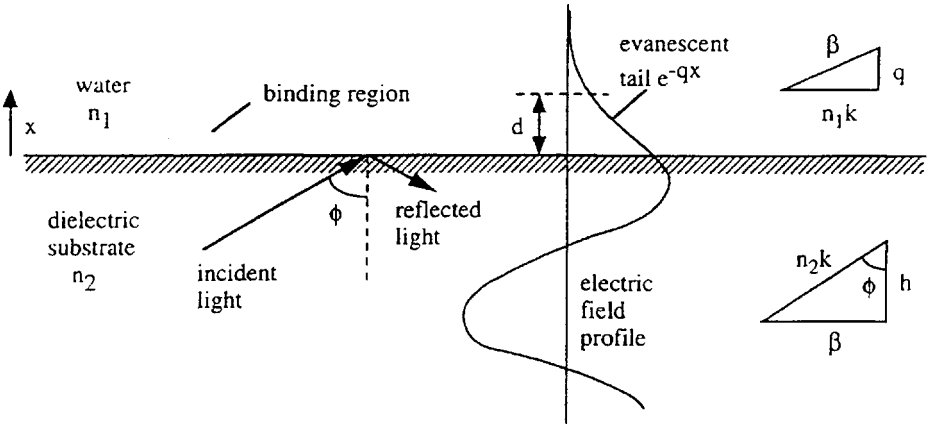

Fig. 1. The configuration for total internal reflection (TIR) of an incident beam from a dielectric with index n_2 onto a medium with index n_1. For angles of incidence exceeding the critical angle ϕ_c, the wave is completely reflected, but a portion of the electric field extends evanescently a distance d into the upper region. The small triangles give the relationships between the propagation constants in the two regions.

$$\beta = n_2 k \sin\phi \tag{2}$$

This relationship, summarized by the lower triangle in Fig. 1, is quadratic:

$$h^2 + \beta^2 = (n_2 k)^2 \tag{3}$$

The electric field in the upper (water) region has a transverse variation of

$$E_1 \propto C\, e^{jQx} \tag{4}$$

where Q is the transverse propagation constant in this upper region. Again, the relationship between propagation constants is given by a quadratic:

$$Q^2 + \beta^2 = (n_1 k)^2 \tag{5}$$

Note, however, as opposed to the lower region where the transverse propagation constant h is properly a real value, under certain important conditions the transverse propagation constant Q can be entirely imaginary. This happens when the angle of incidence ϕ is large enough that β in (5) is greater than $n_1 k$, or from (2)

$$n_2 k \sin\phi \geq n_1 k$$

so

$$\phi \geq \phi_c = \sin^{-1}(n_1/n_2) \tag{6}$$

where ϕ_c is the critical angle (measured with respect to the surface normal) for onset of TIR. Note from (6) that TIR can only occur if $n_2 > n_1$. Then Q can be found from (5):

$$Q = j\sqrt{\beta^2 - (n_1 k)^2} = jq \tag{7}$$

and the electric field in the upper region has the evanescent behavior of exponential decay in the transverse direction:

$$E_1 \propto Ce^{-qx} \tag{8}$$

2.1. Estimate of evanescent penetration depth

The value of q determines the evanescent penetration depth. At position x=d=1/q, the electric field amplitude is reduced to 1/e = 37% of its value at the interface, which is a convenient definition of penetration depth. Equation (7) shows that the exact

value of q depends upon β, which in turn depends upon the angle of incidence (or equivalently the mode number for waveguided light). But as an estimate, for angles somewhat larger than the critical angle, (2) shows that $\beta \approx n_2 k$ and (7) gives

$$q \approx \sqrt{n_2^2 - n_1^2}\, k = (NA) 2\pi/\lambda \tag{9}$$

where NA is the numerical aperture. For a typical interface between a polystyrene (n_2 = 1.59) substrate and a water (n_1 = 1.33) layer, NA = 0.89, and therefore

$$q \approx 5.6/\lambda \tag{10}$$

For incident light of wavelength 633 nm, the corresponding depth of penetration is

$$d = \lambda/5.6 = 113\,\text{nm} \tag{11}$$

The depth given in (11) is sufficiently large to cover a layer of surface-immobilized antibody plus bound antigen, but not deep enough to appreciably interact with proteins in the bulk of the solution. This important attribute of the evanescent field gives biosensors which incorporate TIR the considerable advantage of not requiring a wash step to remove unbound antigen, leading to simpler and quicker assays and to the possibility of real-time measurement of binding dynamics. It is important to note that the evanescent field, though nonpropagating, carries energy from and is coupled to the incident field, and therefore is capable of being absorbed (thus reducing the reflected intensity); of exciting fluorescence in any fluorophores that are within its penetration distance; or of interacting with the index of refraction of various protein layers on the surface. This interaction gives rise to various techniques for detecting protein concentrations described in the remainder of this paper.

3. EXAMPLES OF SENSORS FOR MONITORING SURFACE DYNAMICS

Several groups have developed sensor systems which incorporate evanescent interaction in some fashion or the other. We will mention only a few of these. Surface plasmon resonance (spr) is a phenomenon that occurs when a thin layer (e.g., 50-60 nm) of an optical metal such as silver is deposited on the surface of the transparent substrate in the TIR configuration shown in Fig. 1. The incident beam also must be polarized in the plane of incidence.[3] For a certain angle of incidence (greater than the critical angle), the longitudinal propagation constant of the incident wave will match the longitudinal propagation constant inside the thin metal film, setting up resonant oscillations of electrons inside the film. The periodic bunching of the electrons (plasmons) leads to enhanced surface electric fields, which decay evanescently into the upper solution region and extend over the surface binding layer. At the correct angle of resonance, a major portion of the light intensity is absorbed by the metal (complete absorption is possible for an optimum film thickness) and the corresponding reduction in reflectivity is detected by a photodetector monitoring the reflected beam.

The angle at which a null occurs in the reflected beam intensity is a sensitive measure of the index of refraction of the media above the surface within the evanescent penetration depth. Therefore, this technique can provide essentially real-time monitoring of surface adsorption or binding. The reflectivity null can be detected by either: (1) fixing a narrow incident beam near the reflectivity minimum and monitoring the reflected power; (2) scanning a narrow beam through a range of angles; or (3) sending a broad cone of incident light and using a linear detector. The sensitivity of spr to small changes in refractive index is quite good, with variations of 10^{-5} in index being detectable using the fixed-angle approach.[4] The Pharmacia BIAcore™ sensor is an excellent example of a commercial spr system that is used for a number of surface monitoring applications.[5]

Another device employing evanescent interactions is the resonant mirror biosensor.[6,7] This system uses a sensor with two additional layers located immediately underneath the surface interface in Fig. 1 (with no metal film). A high-index 'resonant' layer (approximately 100 nm thick) forms the interface with the solution, and a lower-index 'coupling' layer (approximately 1 μm thick) lies just beneath the resonant layer. Light of both TM and TE polarization is incident from a transparent prism substrate below both layers, and at a certain angle the light striking the lower layer is coupled through into the upper layer before being reflected downward again. In this condition there is a π phase difference between the two reflected polarizations, which are then made to interfere, producing an output signal that peaks sharply at the angle of resonance. This angle is again very sensitive to the index of refraction within the evanescent distance in the solution region, so the technique provides a real-time capability for monitoring surface binding and interactions. This method has been successfully commercialized as the Fisons IAsys™ resonant mirror device.[8]

In the next sections, the development of waveguiding evanescent immunosensors is described.

4. PLANAR WAVEGUIDE IMMUNOASSAY

The incident beam which is totally reflected from the binding interface in Fig. 1 may be "reused" by trapping it inside a waveguide where it is confined by TIR at both the top and bottom surfaces of the guide. In essence, the beam undergoes repeated bounces as it travels down the guide, and at each reflection from the upper surface, the evanescent tail of the electric field interacts with the surface-bound proteins from the solution, as discussed above. The requirement for waveguiding (i.e., TIR at both surfaces) is that the index of the waveguide, n_2, is greater than those both of the upper region, n_1, and of the region below the guide, n_3. This requirement is easy to meet in practice by using, for example, a polystyrene waveguide (n_2=1.59) with water above (n_1=1.33) and air below (n_3=1.0). In this case the critical angle for cutoff of TIR is $\phi_c = \sin^{-1}(1.33/1.59) = 56.8°$ with respect to the normal at the guide/water interface.

Figure 2 shows a schematic of a waveguide immunoassay system using a sandwich assay format. Laser light is introduced into the waveguide from the left in this figure (either by end coupling or by some other means such as prism or grating coupling[2]). It undergoes repeated bounces down the guide, forming a transverse standing wave pattern for the electric field, corresponding to a certain mode with its associated evanescent tail in the solution region. On the upper surface, capture antibodies have been immobilized. When analyte (such as hCG) is present, it specifically binds to the antibodies. In turn, the bulk solution contains a given concentration of tracer antibodies which bind to additional sites on the bound analyte. These second antibodies have been labeled with a fluorescent molecule (such as Cy5) which is now pulled within the evanescent zone and excited by the waveguided light. Its fluorescent emission is radiated into a broad pattern similar to a dipole radiation pattern; a portion of the emission passes through the waveguide where it can be detected by photodetectors. The waveguide thus acts as a window for the radiated fluorescence. The intensity of the detected fluorescence is related to the concentration of bound antigen, in turn related to the concentration of antigen in the bulk solution.

The use of a waveguide has numerous advantages over single-bounce TIR fluorescence. A major advantage is that it utilizes the exciting light more efficiently by effectively reusing its intensity through multiple bounces. This enhancement factor can be calculated by two methods which give similar results: a full electromagnetic mode theory,[2] or a ray-tracing approximation. Using the ray-tracing approach, it is easy to see why the enhancement factor is inversely proportional to the thickness of the guide, that is, the thinner the guide, the larger the enhancement. For a given angle of incidence inside the guide, a thin guide will have more bounces per unit distance down the guide than will a thick one, and therefore will result in a larger amount of reuse of the incident light energy for a given surface area of bound analyte. Also, the steeper the incident angle (i.e., a smaller ϕ corresponding to a higher mode number), the more number of bounces will occur for a given guide thickness. Therefore, to obtain the largest enhancement factor, a thin guide operating with modes near cutoff should be employed (but not

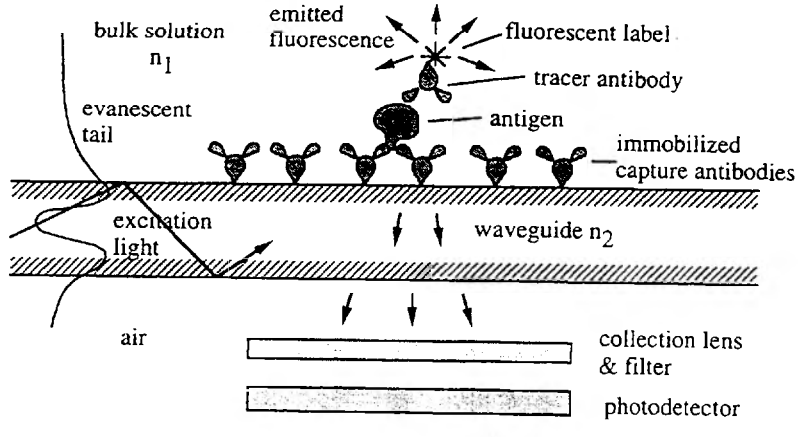

Fig. 2. A schematic representation of the sensing configuration for the planar waveguide immunoassay. When an analyte molecule binds to an immobilized capture antibody, a fluorescently labeled reporter antibody then can also bind and is pulled within the evanescent zone of the waveguided excitation light, thus producing fluorescence.

too close to cutoff since, according to (2), (6), and (7), the evanescent penetration depth goes quickly to infinity at cutoff, eliminating the surface specificity of the sensor, and slight imperfections in the guide can couple higher-order modes into radiating modes, again increasing bulk-solution background fluorescence). These same conclusions can be obtained using a full electromagnetic mode approach by solving for the interfacial electric field amplitude as a function of guide thickness and mode number.

The waveguide can be either round (as in optical fiber sensors) or planar. The use of cylindrical optical fibers in which the fiber core has been stripped of its cladding in the sensing region for exposure to the analyte solution results in sensors which are inherently simple in geometry, convenient for coupling to a laser, and are particularly suited to remote sensing.[9] On the other hand, a planar waveguide has the possibility of employing multiple zones for sensing--such as for on-sensor calibration or for multiple analyte channels--and may be patterned more easily.[10]

Our laboratory has been pursuing development of a planar waveguide immunoassay system for several years. The status of this project is given in the next sections.

4.1. First-generation sensor

The first prototyping system we developed employed a reusable metal flowcell containing a quartz planar waveguide cut from a standard 1 mm-thick quartz microscope slide. The flowcell and optical arrangement are shown in Fig. 3. The flowcell was divided into two channels by means of a low-index Teflon™ gasket next to the waveguide which separated the flowing solution into two compartments. Different solutions were injected into each of the channels: a "sample" solution containing both the analyte and the fluorescently labeled tracer antibody, and a "reference" solution containing only the labeled tracer antibody. This second solution then controlled for both non-specific binding (NSB) and optical fluctuations within the instrument.[11,12]

Light from a red (633 nm) HeNe laser was coupled into the ends of each channel by two cylindrical lenses. The fluorescence from each channel was collected by a single f/5.6 lens and passed to the entrance slit of a 0.25-m grating spectrograph (SPEX Minimate). The output from the spectrograph was detected by a cooled (-44.4 °C) silicon CCD camera (Photometrics series 200). The CCD camera integrated the spectrum for 15s, then the digitized pattern was stored on a Macintosh IIx computer for analysis and display. The output pattern consisted of wavelength information along one axis, and transverse position information (within the longitudinal opening of the entrance slit) along the other axis.

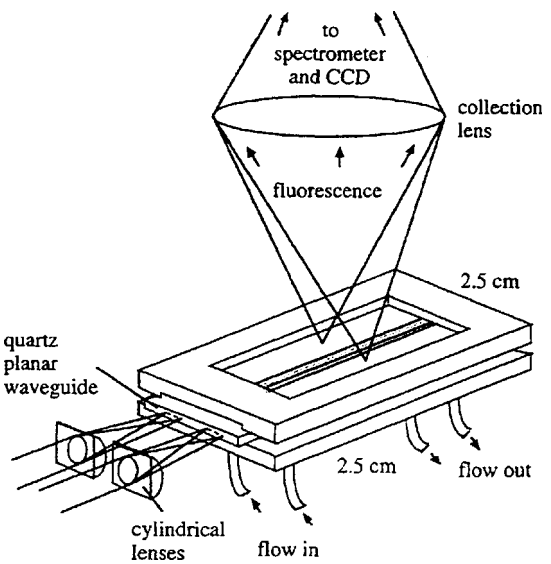

Fig. 3. First-generation planar waveguide sensor, employing a quartz waveguide in a metal flowcell.

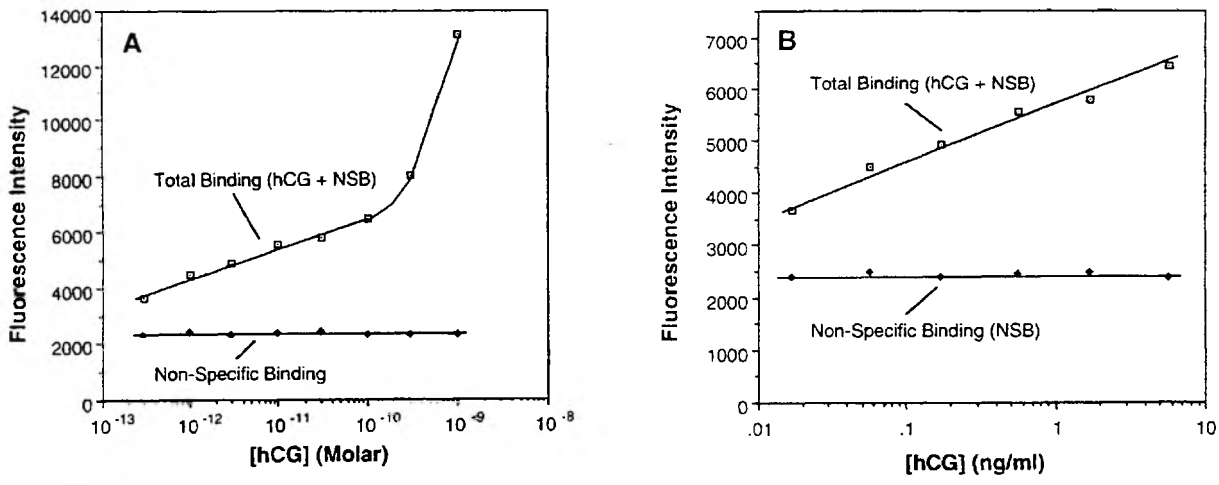

Fig. 4. Binding isotherms for hCG obtained with the first-generation quartz waveguide and flowcell system: (A) Molar concentration scale; (B) ng/ml concentration scale.

Figure 4 shows a binding isotherm that was obtained for human chorionic gonadotrophin (hCG) dissolved in phosphate-buffered saline (PBS) using the first-generation system. A dose-response curve over 3.5 orders of magnitude of hCG concentration (using a molar concentration scale) is shown in panel A, while the response at the low end of the concentration range (this time in units of ng/ml) is shown in panel B. It should be noted that this hCG assay was both rapid (approximately 5 minutes per data point) and homogeneous (no additional reagents or wash steps were required). hCG was chosen as the model analyte because it is measured clinically in the picomolar range and it has become a traditional standard for biosensor development. Note that the lower sensitivity of this system to hCG concentration is in the subpicomolar ($<10^{-12}$ M) range.

4.2. Second-generation sensor

Although the bench-top system described above was a very powerful and flexible tool for prototype development, it was not compact or inexpensive enough for eventual commercial development. We therefore undertook two redesigns: (1) development of an inexpensive, injection-molded plastic sensor to replace the quartz waveguide, metal flowcell and coupling lenses; and (2) fabrication of a compact, inexpensive optics and electronics package to replace the much larger bench apparatus.

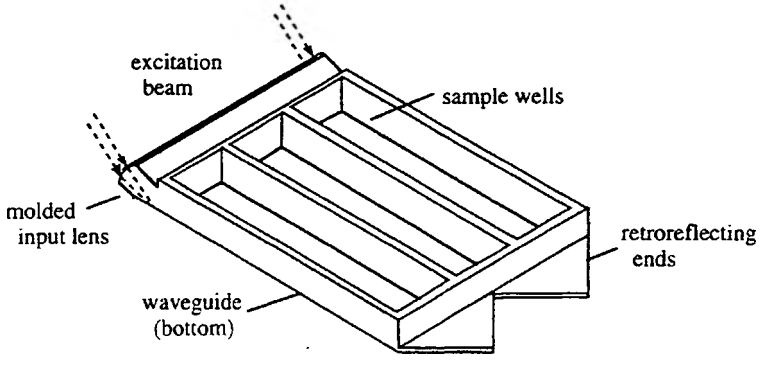

Fig. 5. Second-generation waveguide sensor, consisting of a molded polystyrene waveguide with an integral lens, retroreflecting ends, and three molded sample wells.

The injection-molded sensor design is shown in Fig. 5. It is a one-piece polystyrene unit consisting of a 0.5 mm-thick waveguide on the bottom, an integral coupling lens, and three sample wells on top of the waveguide. The cylindrical coupling lens is molded to the front end of the waveguide to allow greater tolerance in positioning the sensor in the instrument (an important consideration for an inexpensive field instrument). It is angled at a nominal 25° with respect to the waveguide surface in order to promote the coupling of higher-order modes, thus increasing the interfacial electric field intensity and the enhancement factor as discussed earlier. Two 45° retroreflectors are also molded into the far end of the waveguide to reflect (by TIR) the waveguided light back on itself; this theoretically can increase the effective excitation intensity by a factor of up to two.

Sample wells are molded on top of the waveguide to eliminate the need for a flowcell. Three wells are used to enable each sensor to be calibrated on-board. In the present assay scheme, the sample solution (containing the analytes to be tested) is added to one of the wells, while calibration standards are added to the other two. The sensor has an additional feature: Within each well, different zones corresponding to different types of antibodies can be laid out (using coupling chemistries described later). Therefore, with three wells and, say, four types of assays per well, each sensor is actually a 12-channel sensor. Each of these 12 zones has a sensing area of about 0.25 cm^2.

The optical instrumentation employs a 633-nm, 12-mW laser diode as the source. Its output is formed into a sheet beam for coupling into the waveguide by using a pair of cylindrical lenses arranged as a Keplerian beam expander. The fluorescent emission from the sensor is collected by an f/5.6 macrolens, passed through a bandpass filter to reject the elastically scattered laser light, and imaged onto a spatially resolved detection system. This imaging configuration allows separate detection of the signals from each zone.

4.2.1. Immobilization chemistries and experimental results

Before beginning the hCG assays, it was important to first determine whether the new plastic sensor would perform as well as other more traditional assays such as the radioimmunoassay (RIA). One such measure of performance is intrinsic sensitivity, which is defined as the minimum number of immobilized immunoglobulin G (IgG) molecules that can be detected per cm^2 of the sensing surface. This parameter is useful because it is a direct measure of the innate performance of the sensor, independent of the antigen-binding affinity of the antibodies employed in an immunoassay. Intrinsic sensitivity studies were therefore conducted that showed that the polystyrene sensor could detect approximately $3x10^{-17}$ moles cm^{-2} of immobilized IgG that was labeled with the red-emitting cyanine dye Cy5. Using a sensing area of 0.25 cm^2, this corresponds to about 5 million immobilized IgG molecules. In comparison, a typical RIA can detect about $1x10^{-15}$ moles cm^{-2} of immobilized ^{125}I-IgG (150 million IgG molecules per 0.25 cm^2). Thus, the intrinsic sensitivity of the plastic sensor is about 30-fold better than that of a radioimmunoassay.

We next undertook evaluation of the plastic sensor in immunoassays. This involved: (1) development of methods for immobilizing antibodies to specific regions of the polystyrene waveguide; and (2) comparison of immunoassays performed using the first- and second-generation immunosensors.

4.2.1.1. Immobilization Chemistries - As mentioned above, the plastic sensor unit was designed so that up to four different assays could be performed on the same sample. This would be accomplished by immobilizing different types of capture antibodies on different regions of the waveguide, a process referred to as patterning. Two different patterning methods appear suitable for immobilizing antibodies to the polystyrene sensors—liquid jet printing and photolithography. In the former, a machine similar to an ink jet printer is used to spray reagents onto a specific region of the waveguide; in the latter, ultraviolet light is used to photochemically crosslink antibodies to selected regions. We have developed three different immobilization chemistries that are compatible with these patterning strategies.

Before describing these chemistries, brief mention should be made on how they were evaluated. Optical grade polystyrene sheet was cut into 1 cm x 1 cm chips and coated with capture antibodies using a given immobilization chemistry. A monoclonal antibody (9-40) that binds the hapten fluorescein was used as the capture antibody. Radioimmunoassays were then conducted using two different analytes—bovine serum albumin labeled with ^{125}I (^{125}I-BSA) and bovine serum albumin double-labeled with fluorescein and ^{125}I [Fl-(^{125}I)-BSA]. The results of these assays are shown in Table I. Bovine serum albumin is inherently surface-active and adsorbs strongly to polystyrene. Thus, it is an excellent protein for evaluating non-specific binding in immunoassays. Because the immobilized capture antibody will only bind specifically to Fl-(^{125}I)-BSA, both specific and non-specific binding can be determined by comparing the amounts of Fl-(^{125}I)-BSA and ^{125}I-BSA that bind to the polystyrene

chips for each of the three chemistries (see Table I).

The first immobilization chemistry is based on physical adsorption of antibodies to the waveguide. The University of Utah has licensed to a private company a method in which the antibody is briefly exposed to acidic conditions just prior to immobilization. It has been shown[13-16] that this acid pretreatment step improves the antigen-binding capacity (AgBC) of immobilized antibodies by up to 3-fold in some cases. This immobilization chemistry is relatively simple and compatible with liquid jet printing technology, but as shown in Table I, it exhibits a higher degree of non-specific binding (approximately 16% of total binding) than the other methods.

The other two immobilization chemistries are based on a family of tri-block polymers of the form PEO-PPO-PEO, where PEO stands for poly(ethylene oxide) and PPO stands for poly(propylene oxide). These surfactants are sold under the trade name *pluronics* and come in a variety of chain lengths for both the PEO and PPO blocks. The PPO block is significantly more hydrophobic than the PEO blocks and adsorbs readily to non-polar surfaces such as polystyrene, leaving the PEO blocks exposed to bulk solution. The free ends of the PEO chains exhibit high mobility, literally sweeping proteins away from the surface. As shown in Table I, when the polystyrene surfaces were coated with pluronics (without capture antibody), no detectable binding of either ^{125}I-BSA or Fl-(^{125}I)-BSA was observed.

Table I—Evaluation of Different Immobilization Chemistries

Surface	Capture Antibody[d]	Crosslinker[e]	Total Binding[f] (moles/cm^2) x10^{-13}	Non-specific Binding[g] (moles/cm^2) x10^{-13}	Percent Non-specific Binding[h] (%)
PS[a]	None	None	19.6	15.3	~100
PS	APT IgG	None	4.86	0.784	16.1
PS/F108[b]	None	None	< 0.01	< 0.01	~100
PS/F108	Fab'	BPM	3.86	0.057	1.5
PS/F108	Fab'	BPIA	10.1	1.95	19.0
PS/P105[c]	None	None	< 0.01	< 0.01	~100
PS/P105	Fab'	BPM	3.66	< 0.01	< 0.3
PS/P105	Fab'	BPIA	6.78	0.039	0.6

[a]PS—polystyrene surface

[b]PS/F108—polystyrene surfaces were coated with pluronics F108, a tri-block polymer with the structure: EO_{129}-PO_{56}-EO_{129}, where EO and PO are ethyleneoxide and propyleneoxide, respectively). The PPO block adsorbs to hydrophobic surfaces leaving the two PEG blocks exposed to bulk solution.

[c]PS/P105—polystyrene surfaces were coated with pluronics P105, a tri-block polymer with the structure: EO_{39}-PO_{56}-EO_{39}.

[d]Capture antibody—APT IgG: acid pretreated 9-40 IgG (9-40 is a monoclonal antibody that binds the fluorescein hapten); Fab': antigen-binding fragment of the 9-40 IgG.

[e]Crosslinker—BPM: benzophenone maleimide; BPIA: benzophenone iodoacetamide.

[f]Total binding—amount of antigen that bound to an antibody-coated silica surface after 1 hr exposure to a saturating concentration of fluorescein-(^{125}I)-BSA (includes both specific and non-specific binding).

[g]Non-specific binding—amount of ^{125}I-BSA that bound to an antibody-coated silica surface after 1 hr exposure to a saturating concentration of the same (includes only non-specific binding).

[h]Percent non-specific binding—ratio of non-specific binding to total binding.

In both the second and third immobilization chemistries, the surface of the waveguide is coated with pluronics before attachment of antibodies, but the two chemistries differ in how the antibodies are attached. In the second chemistry a photochemical crosslinking agent is used to conjugate antigen-binding fragments (Fab') to the PEO blocks, making this method suitable for patterning by photolithography. In the third chemistry Fab' fragments are attached to pluronics using a chemical crosslinking agent, making this method compatible with liquid jet patterning. The photochemical crosslinking method was evaluated with two different pluronics (F108 & P105) and two different photochemical crosslinkers (BPM and BPIA). These results are presented in Table I and show that while acceptable levels of total antigen binding can be obtained with all four pairwise combinations, an unacceptable level of NSB (about 20% of total binding) is obtained when antibodies are immobilized to F108 using the BPIA crosslinker. The other three pairwise combinations give very low levels of NSB ($\leq$ 1.5% of total binding). Furthermore, the P105/BPM pair was especially good, giving an undetectable level of NSB.

4.2.1.2. hCG Immunoassay Results - A series of immunoassays was then conducted with the polystyrene sensors using hCG as the analyte; the results are shown in Fig. 6. The first two immobilization chemistries described above were evaluated—physical adsorption of IgG (either native or acid-pretreated) (Fig. 6, panel A), and conjugation of Fab' fragments to immobilized pluronics F108 using crosslinkers (Fig. 6, panel B). Similar experiments were performed for each immobilization method. Different concentrations of hCG (0.0 M, 10^{-12} M, and 10^{-8} M, prepared in PBS) were added to the three sample wells of the plastic waveguide (each well also received a 10^{-9} M concentration of Cy5-labeled tracer antibody), and fluorescence intensity was measured as a function of time. In Fig. 6, the lower curves obtained in the absence of hCG reflect the non-specific binding of the tracer antibody to the waveguide. As expected, a lower degree of NSB is observed for the second immobilization method (pluronics) than for the first (physical adsorption). Furthermore, distinct curves are obtained for 0.0 M and 10^{-12} M concentrations of hCG (using either immobilization method), which suggests that the sensitivity of the assay is close to 10^{-12} M and that meaningful data can be obtained in a five-minute assay period.

5. CONCLUSIONS

Evanescent-based biosensors are valuable devices for detecting surface binding events rapidly without requiring a wash step. By employing an optical waveguide as the solid-phase support, the excitation light is effectively enhanced. In our laboratory, a first-generation planar waveguide sensor employing a quartz waveguide in a metal flowcell has achieved a sensitivity of below 10^{-12} M for the analyte hCG (see Fig. 4). The second-generation sensor, consisting of a 0.5-mm thick molded polystyrene waveguide with integral lens and multiple wells, produced immunoassay results which show a sensitivity of about 10^{-12} M for hCG (see Fig. 6). Further improvements in sensitivity are expected to be achieved with increased optical excitation efficiency, better detection, and improved antibody binding properties.

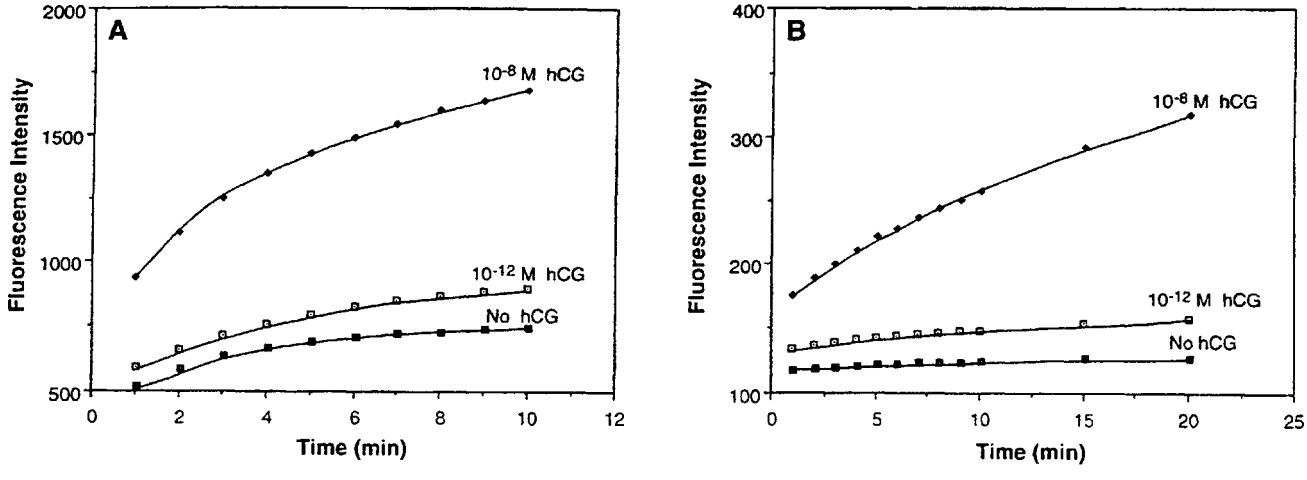

Fig. 6. Comparison of binding using the second-generation polystyrene sensor with two different immobilization chemistries: (A) Physical adsorption; (B) Pluronics F108 with chemical crosslinker.

A thin-film version of this device has also been developed[17] which exhibits even lower sensitivity, mostly due to its dramatically thinner waveguide. The guide is fabricated by depositing a 1 μm-thick siliconoxynitride layer on a quartz substrate using a plasma-assisted chemical vapor deposition technique, a procedure available in most integrated circuit fabrication facilities.

6. ACKNOWLEDGEMENTS

Portions of this research were sponsored by AKZO America, Inc. and HCP Diagnostics, L.P., whose support is gratefully appreciated. Some of the technology reported herein is subject to patent applications assigned to the University of Utah Research Foundation and licensed to a private company.

7. REFERENCES

1. R.P. Buck, W.E. Hatfield, M. Umana and E.F. Bowden, eds., *Biosensor Technology: Fundamentals and Applications*, Marcel Dekker, New York, 1990.
2. R.G. Hunsperger, *Integrated Optics: Theory and Technology*, 3rd edition, Springer-Verlag, Berlin, 1991.
3. H. Raether, *Surface Plasmons on Smooth and Rough Surfaces and on Gratings*, Springer Tracts in Modern Physics, Vol. 111, Springer-Verlag, Berlin., 1988.
4. B. Liedberg, C. Nylander and I. Lundstrom, "Surface plasmon resonance for gas detection and biosensing," *Sensors and Actuators* **4**, 299-304, 1983.
5. B. Liedberg, I. Lundstrom and E. Stenberg, "Principles of biosensing with an extended coupling matrix and surface plasmon resonance,"*Sensors and Actuators B* **11**, 63-72, 1993.
6. R. Cush, J.M. Cronin, W.J. Stewart, C.H. Maule, J. Molloy and N.J. Goddard, "The resonant mirror: a novel optical biosensor for direct sensing of biomolecular interactions - Part I: Principle of operation and associated instrumentation," *Biosensors & Bioelectronics* **8**, 347-353, 1993.
7. P.E. Buckle, R.J. Davies, T. Kinning, D. Yeung, P.R. Edwards and D. Pollard-Knight, "The resonant mirror: a novel optical sensor for direct sensing of biomolecular interactions - Part II: Applications," *Biosensors & Bioelectronics* **8**, 355-363, 1993.
8. R.J. Davies and D. Pollard-Knight, "An optical biosensor system for molecular interaction studies," *American Biotechnology Laboratory*, July, 1993.
9. L.C. Shriver-Lake, J.P. Golden, G. Patonay, N. Narayanan and F.S. Ligler, "Use of three longer-wavelength fluorophores with the fiber-optic biosensor," *Sensors and Actuators B* **29**, 25-30, 1995.
10. G. Robinson, "The commercial development of planar optical biosensors, "*Sensors and Actuators B* **29**, 31-36, 1995.
11. J.N. Herron, D.A. Christensen, V. Hlady, V. Janatova, H.-K. Wang and A.-P. Wei, "Fluorescent immunosensors using planar waveguides," in: *Advances in Fluorescence Sensing Technology* (J. R. Lakowicz and R. B. Thompson, eds.) pp. 28-39, SPIE, Bellingham, WA, 1993.
12. D.A. Christensen, S. Dyer, D. Fowers and J. Herron, "Analysis of excitation and collection geometries for planar waveguide immunosensors," in: *Fiber Optic Sensors in Medical Diagnostics* (F. P. Milanovich, ed.) pp. 2-8, SPIE, Bellingham, WA, 1993.
13. J.-N. Lin, J.D. Andrade and I.-N. Chang, "The influence of adsorption of native and modified antibodies on their activity," *Journal of Immunological Methods* **125**, 67-77, 1989.
14. J.-N. Lin, I.-N. Chang, J.D. Andrade, J. N. Herron and D. A. Christensen, "Comparison of site-specific coupling chemistry for antibody immobilization on different solid supports," *J. Chromatography* **542**, 41-54, 1991.
15. I.-N. Chang, J.-N. Lin, J.D. Andrade and J.N. Herron, "Adsorption mechanism of acid pre-treated antibodies on dichlorodimethylsilane-treated silica surfaces," *J. Colloid Interface Sci.*, July, 1995.
16. I.-N. Chang and J.N. Herron, "Orientation of acid pretreated antibodies on hydrophobic dichlorodimethylsilane-treated silica surfaces," *Langmuir*, July, 1995.
17. T.E. Plowman, W.M. Reichert, C.R. Peters, H.-K. Wang, D.A. Christensen and J.N. Herron, "Femtomolar sensitivity using a dual channel thin film integrated optical waveguide fluoroimmunosensor," *Biosensors and Bioelectronics,* in press.